Hindawi
Geofluids
Volume 2022, Article ID 8313048, 15 pages
https://doi.org/10.1155/2022/8313048

Research Article

Prospect Analysis of Paleocene Coalbed Methane: A Case Study of Hangu Formation, Trans-Indus Ranges, Pakistan

Hamza Azam Qadri,[1] Ali Wahid,[1] Numair Ahmed Siddiqui,[2] Syed Haroon Ali,[3] Ahmed Abd El Aal,[4,5] Amirul Qhalis Bin Abu Rashid,[2] and Mohd Najib Bin Temizi[2]

[1]*Institute of Geology, University of Azad Jammu and Kashmir, Muzaffarabad, Azad Kashmir 13100, Pakistan*
[2]*Department of Petroleum Geoscience, Universiti Teknologi Petronas, Seri Iskandar, 32610 Tronoh, Perak, Malaysia*
[3]*Department of Earth Sciences, University of Sargodha, Punjab 40100, Pakistan*
[4]*Geology Department, Faculty of Science, Al Azhar University, Assiut Branch, Assiut, Egypt*
[5]*Civil Engineering Department, College of Engineering, Najran University, Najran, Saudi Arabia*

Correspondence should be addressed to Ali Wahid; ali.wahid@ajku.edu.pk
and Numair Ahmed Siddiqui; numair.siddiqui@utp.edu.my

Received 22 June 2022; Revised 21 October 2022; Accepted 27 October 2022; Published 12 November 2022

Academic Editor: Dan Ma

The methane trapped in the coal seams has emerged as an unconventional clean energy resource worldwide in this century. The proximate composition, ultimate content, cleat structure, porosity type, and pore structures are the debatable components for its trapping mechanism. Further, the brittle and ductile properties of minerals influence in the extraction of the methane from the coal seams. In this research, Coalbed methane prospect is demonstrated by analysing the Hangu Formation's coal seam of Trans-Indus Ranges, Pakistan. This case study is helpful to find the occurrence, trapping ability, and methane extraction capacity in its cleat structures and pores. A number of samples were tested from the different coal mines in terms of these debatable components. The results indicate that the rank of studied coal is bituminous to subbituminous in which the carbon ratio, volatile matter, and sulfur contents are increasing with depth towards the south. The transitional connected face and butt cleats are partially filled with minerals and the intergranular, dissolved, and tissue pore types are also identified in it. It can be helpful for the occurrence, migration, and trapping of methane. Furthermore, the higher surface areas and cumulative pore volumes enhance the capacity of gas adsorption with depth in the study area. Moreover, the increasing brittle minerals in the coal composition towards the south can be helpful for the fracking of coal seams for economical gas extraction. It is suggested that this workflow can be implemented in any region with same coal rank and cleat types.

1. Introduction

Worldwide, the Coalbed Methane (CBM) is known as the unconventional energy resource which consists of mainly methane that trapped in coal seams during the coal formation. [1]. For the past 22 years, CBM is considered a significant energy resource globally as it is cost-effective and emits less CO_2 per unit of energy as compared to the combustion of coal, oil, or even wood [2]. To overcome the world's energy demand, the extraction of economic methane which is trapped in coal seam is necessary. The United States, Russia, China, Australia, United Kingdom, Germany, and others contain approximately 30,000 TCF of gas trapped in vast coal deposits [3]. The coal seam of shallow depth of Bowen Basin, Australia, has been drilled with over 500 wells and has an estimated annual production of 100 BCF. Similarly, the CBM industry in China is also growing and has an estimated production of 130 BCF per year [4]. On the other hand, Canada did not reach its full potential for CBM extraction but still, Alberta consists of almost 3500 CBM wells and produces 100 BCF (annually) of methane from bituminous to low volatile coal [5]. In the US, the San Juan Basin and Powder River Basin consists of low to high volatile bituminous rank coal and producing methane [3].

The coal seams mostly consist of moisture, organic matter, and mineral matter. These contents are trapped in the cleat structures having a complex pore system [6–8]. The coal is determined into four ranks including lignite, subbituminous, bituminous, and anthracite ordered from lowest to high rank, respectively. Bituminous coal is considered as the maximum capacity to adsorb economical methane [9]. The methane (CH_4) in the subsurface coal seams is trapped in the cleat structures and adsorbed in the pores of coals. These cleat structures are formed due to the development of natural fractures, whereas the micropores present in these seams are responsible for the generation of porosity and permeability [10]. Moreover, the cleat structures (fractures) and the porosity including the pore connectivity and pore throat size are important features for accumulation of unconventional reservoirs [11]. These features generate the permeability which increases with time and act as the pathways within the reservoir [12, 13]. However, the higher brittle minerals are ideal for artificially induced fractures and help in less energy loss for the extraction of methane [14–17].

Pakistan is suffering from a shortfall of energy and consistent efforts are needed to exploit the new economic resources [18]. The country has one of the largest coal reserves in the world which consists of more than 186282 million tons (Mt) [19]. The extraction of methane from the coal seams can be an important solution to fulfill the energy demands. In this research, the coal seam of the Hangu Formation (Paleocene age) of Trans-Indus Ranges are studied to find their potential to act as coalbed methane. The gross calorific value of Makarwal coalfield ranges between 10500-14000 (Btu/lb) which almost ranges to the heating value of productive coalbed methane of Illinois bituminous (12770 Btu/lb) and Wyoming subbituminous (8683 Btu/lb) of Powder River Basin [20]. It is believed that the methane is trapped in the coal seams of the Hangu Formation which was identified during the Kuch iron exploratory tunnel and caused the losses in an explosion at the tunnel. The flammable gas is also identified during drilling at Chichali Pass with artesian water in Hangu Formation which is believed to trap along the faults in the study area [21]. The extensive tectonic activities resulting in folding and faulting [22–26] are the cause of the thermal maturity of coal seams [27]. Keep this in mind, the objectives of this research are to find the rank of Hangu Formation coal and the internal cleat structures to identify its type, retention, and flow of methane. Further, the type of porosity (dual porosity) and pore structure of coal is also studied to understand the adsorption capacity of methane, whereas the mineralogical identification is studied to find the brittle minerals in the coal of the Hangu Formation to investigate its potential for methane extraction in the study area.

2. Study Area and Geological Setting

This case study was conducted at Makarwal coalfield in Mianwali district, Punjab, Pakistan (Figures 1(a) and 1(b)). The coalfield was mined as early as 1903 and plays an important role in energy resources and manufacturing by-products [28]. The total reserves of Makarwal and neighboring Salt Range coalfields are about 235 Mt, in which the measured reserves are 57 Mt [19]. The depth of the coal reserves above the sea level is 450 m which includes the mineable reserves [29], whereas the working depth of coal mines is up to 300 m above sea level and designated the reserves of 7.5 Mt below; whereas, from the altitude of 300 m to 600 m inferred reserves are 9.2 Mt [28].

Geologically, the Makarwal coalfield consists of a sinuous fold and thrust belt, located in the Surghar Range of Trans-Indus Ranges, Pakistan (Figure 1(a)). These ranges consist of Kalabagh hills, Surghar-Shinghar Ranges, Marwat-Khisore Ranges, and the Pezu-Bhitani Range. It is bounded by the Kohat Plateau in the north, Punjab Foreland in the south, whereas the Indus River forms its eastern boundary and its western part is bounded by Sulaiman Range [33]. The Kalabagh hills are situated in the eastern part of the Trans-Indus Ranges and consist of a structural transect of Surghar Range. The Kalabagh Fault (KF) is situated in the eastern part and formed due to transpressive right-lateral strike-slip movement in Northern Pakistan [34–37], whereas the Marwat-Khisore Ranges bound the Bannu Basin in the south and characterize by east-west to east-northeast structural trends. Furthermore, the Pezu-Bhitani Range is the westernmost surface expression of the Trans-Indus Ranges and formed the northeastern extension of the Sulaiman Ranges [38]. Regionally, these events are representing the tectonic impact due to the Himalayan orogeny towards the north of the study area [21]. The Surghar Range is shoe-shaped south-plunging anticlinal structure (Figure 1(a)) with a series of ridges bounded by the Indus River. The range consists of an east-west structural trend along the southern margin of the Kohat Plateau, whereas it is transformed into a north-south trend along the eastern flank of Bannu Basin [33]. The Surghar Anticline is detached at the base of the Jurassic sequence in which the forelimb of the anticline is characterized by a south-verging thrust [39]. The stratigraphy of the Trans-Indus Ranges consists of marine and nonmarine sources of sedimentary rocks ranging from Permian to Pleistocene sequences which are exposed along with these ranges due to compressional tectonics [28]. The exposed stratigraphic succession in the Surghar Range comprised of Musa Khel group, Baroch group, Surghar group, Makarwal group, Cherat group, and Siwaliks group ranging from Triassic to Miocene/Pliocene age [38].

This research is conducted on Hangu Formation Paleocene age coal of Makarwal group [39]. It has a lower unconformable contact with the Lumshiwal Formation of Cretaceous age and upper contact with the conformable Lockhart Formation [40]. The Hangu Formation mainly consists of interbedded shaly sandstone, coal, interbedded shale and siltstone, and carbonaceous shale (Figure 1(c)). Overall, the sedimentary structures and lithology is indicating a shallow marine and deltaic depositional environment [21]. The laterite exposure at the base of the Hangu Formation indicates the break in the deposition. Hence, the laterite specified the higher exposure to varying weathering environments [41]. The coal, carbonaceous shale, and interbedded shaly sandstone overlie the laterite. The coal seam (almost 2 m) is identified above the carbonaceous shale in the lower

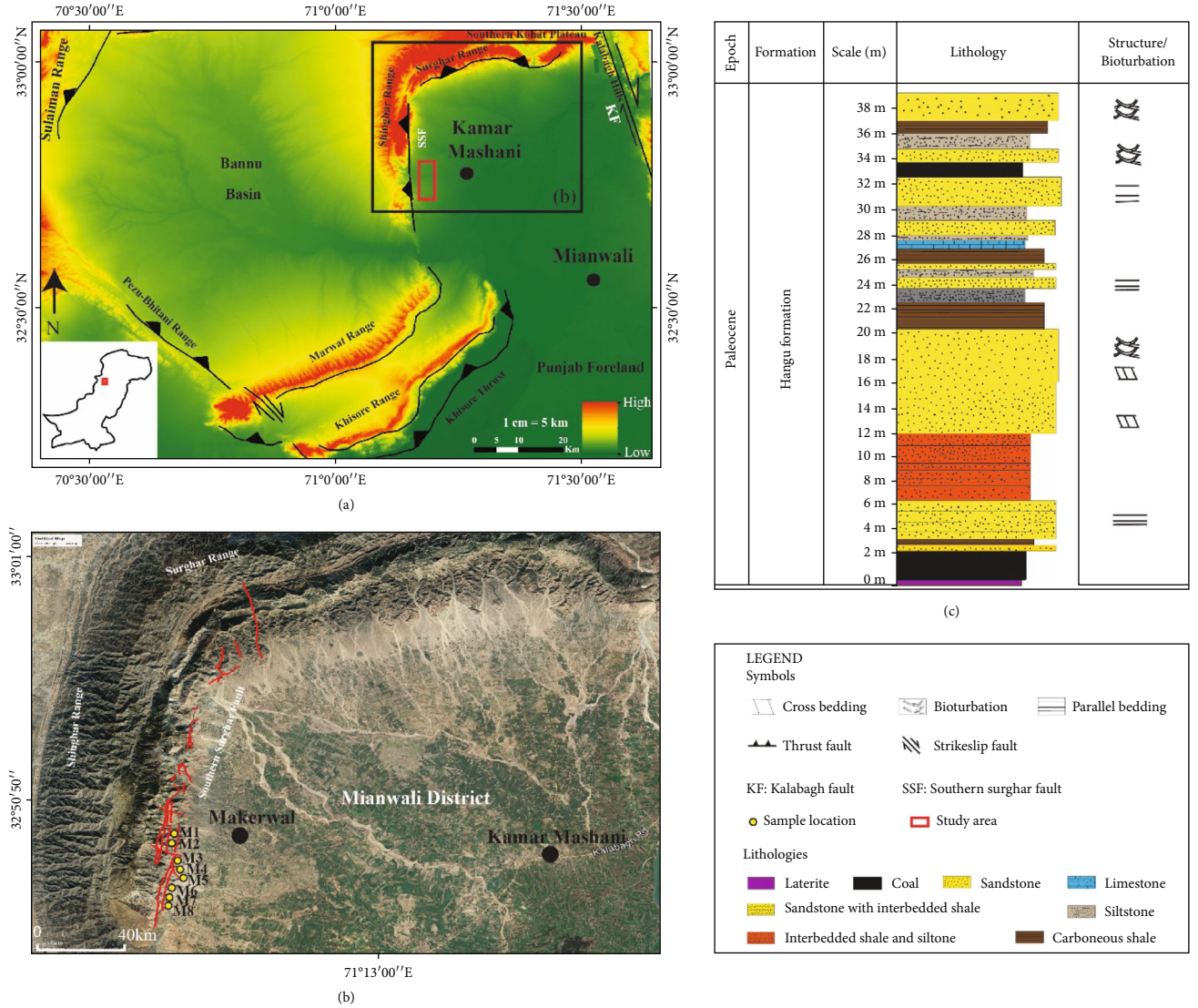

Figure 1: The tectonic map of the Trans-Indus Ranges (a) geographic location of Makarwal coalfield indicating sample locations (b) (modified from [29–32]), lithostratigraphy of the Paleocene Hangu Formation (c) in the study area.

part of the Hangu Formation. Meanwhile, the upper part also consists of a coal seam with less thickness bounded by sandstone beds. It is indicated that the coal was deposited in a humid vegetated swamp area. Hence, it is the ultimate environment for the deposition of coal and carbonaceous shale [42]; whereas the sandstone is medium to thick-bedded and consists of cross-bedding and bioturbation. It is indicating the fining upward sequence deposited in high-energy fluvial settings. The high bioturbation in the upper part of the Hangu Formation is showing a tidal flat environment [43]. The Hangu Formation coal exposures are situated on the east scarp gradient of the Surghar Range which is situated at its south-western extremity [44]. The coal is also mapped and extracted from the western limb on the subsurface on the eastern plain. The thickness of the exposed Hangu Formation is variable (2 feet to 10 feet) from north to south. However, the average coal strata thickness is 4 feet [45]. Generally, the Makarwal Anticline contains the majority of coal and dip 30 W. The rank of coal is high volatile subbituminous [45]. This research is an addition to the evaluation of the CBM resources in the coal seam of the Hangu Formation.

3. Materials and Methods

The methodology used for this research mainly consists of field and laboratory work. In the field study, the coal samples of the 8 mines were collected at different depths of the Makarwal coalfield. The sampling of the coal was based on the procedures set in the American Society for Testing and Materials specifications (ASTM, 1967, D388-66) [46]. The overall 40 samples (5 samples from each mine) of the coal seam were collected and stored in the gunny bags to avoid the loss of moisture content in the samples. In this study, the two representative samples of each mine were used. The representativeness of these samples are based on the fresh coal samples which do not have the exposed weathered surface and loss of moisture content for the laboratory

analysis. Further, the coordinates of each coal mine location were marked to understand coalbed methane response based on its lateral thickness with depth as the thickness of the Hangu Formation coal is increasing with depth.

The laboratory work includes the proximate and ultimate analysis, Scanning Electron Microscope (SEM) analysis, Energy Dispersive X-ray Spectroscopy (EDX) analysis, Pore size analysis, and X-ray Diffraction Spectroscopy (XRD) analysis. For the proximate and ultimate analysis, the 16 representative coal samples were prepared by grinding the samples into a powdered form that can easily pass through the mesh size of 60 numbers. The proximate and ultimate analyses were majorly used to find the rank of coal. Specifically, the proximate analysis was conducted to identify the content of carbon as compared to the moisture content, volatile matter and ash content within the coal samples. The moisture content is based on the mass loss of each sample after heating in a seven-moisture oven, whereas the fixed carbon content was evaluated from the solid combustion residue after heating the coal sample in which the volatile matter has been discarded. Similarly, the volatile matter was also measured in a fluid furnace that works at 1000° C, as it is one of the most commonly measured coal parameters [47]. It has the reverse trend of solid carbon. The amount of fixed carbon that exists in a coal sample was determined by nonvolatile carbon. The ash content is closely linked to the potential for methane adsorption and it is also known as coal combustion residuals. It was determined by calculating the amount of material left after the burning of coal in the ash stove at almost 750°C. On the other hand, the ultimate analysis was used to identify the elemental composition of coal in which the major carbon elements were compared to hydrogen, sulfur, nitrogen, and oxygen [48, 49]. While the total oxygen and ash contents were calculated according to the ASTM standards (D3176-09), in comparison to noncombustible ash of coal, the overall oxygen content is the primary constituent of the five main elements of carbon, hydrogen, oxygen, nitrogen, and sulfur.

The SEM analysis and EDX analysis were performed by placing the sample in a solid form inside the JSM-5910 electron microscope having tool INCA-200. The resolving power was 2.3 nm and the zooming capacity was 30000x and maximum at an accelerating voltage of 30 k. It helped to find the cleat patterns in the coal samples, whereas the EDX was used for the detection and quantification of filling elements within these cleat patterns [48]. For the surface area and pore size identification of the solid coal samples, the pore size analyzer, namely, Micromeritics ASAP 2020 was used to identify the type of pores, pore volume, and surface area. For this purpose, the samples were kept in the atmosphere for extraction of moisture and cooled in vacuum conditions. Further, the nitrogen (N_2) gas was injected into the samples to identify the adsorption capacity in the pores of coal samples in the equipment [50]. Hence, gas adsorption is a well-established tool for the characterization of the available surface area and its capacity to absorb the methane. The surface area of coal was measured by the Brunauer, Emmett, and Teller (BET) method by using the Equations (1) and (2), whereas the Barrett, Joyner, and Halenda (BJH) model was used to find the porosity and pore volume by using the Equation (3), [51].

$$\frac{p^o/\mathrm{prO}}{V_{\mathrm{tot}}(1-(p/pO))} = \frac{1}{V_{\mathrm{mon}}C_{\mathrm{ad}}} + \frac{C_{\mathrm{ad}}-1p}{V_m C_{\mathrm{ad}}\, prO}, \tag{1}$$

$$S_{\mathrm{area}} = \frac{V_{\mathrm{mon}}N_{\mathrm{av}}A_{\mathrm{nitm_{sam}}}}{2240m}, \tag{2}$$

$$r_k = -\frac{v_v}{\mathrm{RTln}\,(p^o/\mathrm{prO})}, \tag{3}$$

Where p^o/pr0 is the relative pressure; V_{tot} is the total volume of adsorbed nitrogen (cm^3/g); V_{mon} is the monolayer amount of gas adsorbed (cm^3/g); C_{ad} is the constant related to adsorption; S_{area} is the specific surface area (m^2g); N_{av} is the Avogadro constant (6.02×10^{23}); A_{nit} is the nitrogen molecule surface area (m^2); m_{sam} is the weight of the coal sample (g); r_k is the Kelvin radius (m); V_v is the molar volume (L/mol); and γ is the surface tension (N/m).

For the XRD analysis, the solid coal samples were converted into powder form, and the detection process was performed to identify the ductile and brittle minerals in coal samples. The test conditions were as follows: temperature 25°C, 50 percent (%) relative humidity, the target made of copper (Cu), 40 kV voltage of X-ray tube, current 40 mA, minimum scanning step size 0.001° (2θ), and minimum step size omega 0.001°. The peaks generated from XRD analysis were used for the identification of the minerals through the height (cts), pos. (°2Th.), and d-spacing [52]. The percentage of different minerals (clay, brittle mineral) was acquired from the data intensity of each sample obtained from XRD analysis. For the interpretation of the XRD results, the Origin© software was used to generate the peaks of different minerals.

4. Results and Discussions

4.1. Coal Rank Identification. The methane trapped in the coal seam is majorly dependent upon the quality of coal. Hence, the different rank of coals has different sorption capacity. The sorption capacity and rank of Hangu Formation coal were identified based on proximate and ultimate analysis. From mines M1 to M3, the thickness of coal seams is varied by approximately 2-5 m in shallow depth. However, from the mines M4 to M8, it varies up to 8-10 m towards the south of the study area. The proximate analysis indicates that the coal samples of shallow depth mines (M1-M2) have a moisture content of almost 25% (average), which is decreasing with the thickness and depth towards the south. In the deeper section, from M3 mine, it decreases by almost 6% (Figure 2), whereas the identified volatile matter is 35% (avg.) in the shallow depth mines and has a maximum value of 45% in the deeper depth mines (M3-M8). Overall, the increased ratio of volatile matter is identified from the M2S2 sample of M2 mine which reached up to 42%. However, the fixed carbon in the M1 mine is almost 23%, and it is increasing towards the deeper part of the Hangu Formation. The fixed carbon ratio in the deeper mines has an

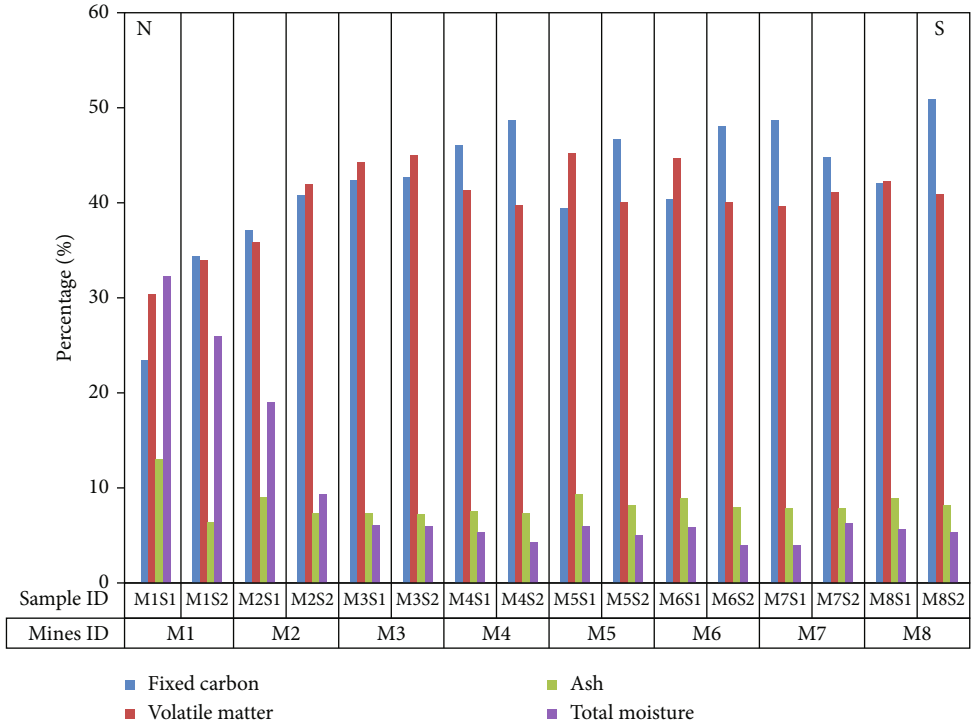

FIGURE 2: The proximate analysis to indicate the fixed carbon, volatile matter, ash content, and total moisture in coal samples. The proximate analysis from mines (M1-M8) indicating the increase in fixed carbon and volatile matter and decrease in ash and total moisture content towards the south of the study area.

average ratio of 45%. Moreover, the shallower depth coal mine (M1) consists of almost 13% ash content which has a decreasing trend of 8% (average) towards the deeper depth (Figure 2). It is interpreted that the higher moisture content identified in the shallow depth mines indicates the lower sorption capacity of gases, which in turn, can reduce the flow of gas; whereas, in the deeper mines, the lower and equilibrium moisture content can increase the gas sorption capacity of Hangu Formation coal seam. Similarly, the higher carbon content and volatile matter with a decrease in ash content with the depth indicates the good gas sorption capacity in the deeper mines (Figure 2).

The ultimate analysis is based on the elemental composition of the carbon, hydrogen, oxygen, sulfur, and nitrogen identified in the coal samples of different mines (Figure 3). Overall, the carbon content in all the samples of the mine varies from 49 to 60.25%. However, the hydrogen varies between 8.89 and 4.84% in all the samples. The higher carbon content and lower hydrogen content in the studied samples are indicating the higher gas adsorption capacity. Hence, the higher hydrogen has a negative impact on the sorption capacity of methane [53]. It is interpreted that the lower hydrogen content enhanced the gas adsorption capacity in Hangu Formation coal in the study area. Furthermore, the oxygen content in the study samples ranges from 26 to34.24%. The higher oxygen content has a depressing effect on the capacity of methane adsorption in the coal seams [7]. The sulfur percentage is high and ranges between 2.74 and 4.75%. The higher sulfur percentages of coal also indicate the existence of methane content trapped.

Based on the above analysis, it is interpreted that the Hangu Formation coal in the study area can adsorb gas, whereas the deeper mines have ideal conditions to trap methane. Furthermore, the ultimate and proximate values (ASTM standards) are indicating the rank of Hangu Formation coal is bituminous to subbituminous. Bituminous coal has good storage capabilities and can contain methane [54]. Hence, the bituminous coal is not less compacted (intermediate rank coal) as compared to the anthracite rank and can generate good internal structure and adsorb gases due to the possibility of open spaces for gas storage.

4.2. Internal Structure and Mineralization within the Coal. The internal cleat structures and mineral content filled within these cleats of the coal seam of the Hangu Formation were interpreted to understand the generation, migration, and trapping of methane in the studied formation. The samples majorly consist of both face and butt cleats having medium interconnectivity in all the analyzed samples (Figure 4). The face cleats are more continuous as compared to the butt cleats. Further, the butt cleats are of a shorter extent and are perpendicular to the face cleats. Precisely, the I2 irregular reticular cleat subpattern is identified in all the samples. The samples collected at shallow depth consist of both the micro- and macrocleats (Figures 4(a)–4(d)). However, the samples of deeper depth consist of a majorly S-type cleat pattern (Figures 4(e)–4(h)). The multiple microscopic pores are also identified in the samples. The pores in the coal are divided into four classes and different types [55, 56] based on genetic type classification. In the study area, the

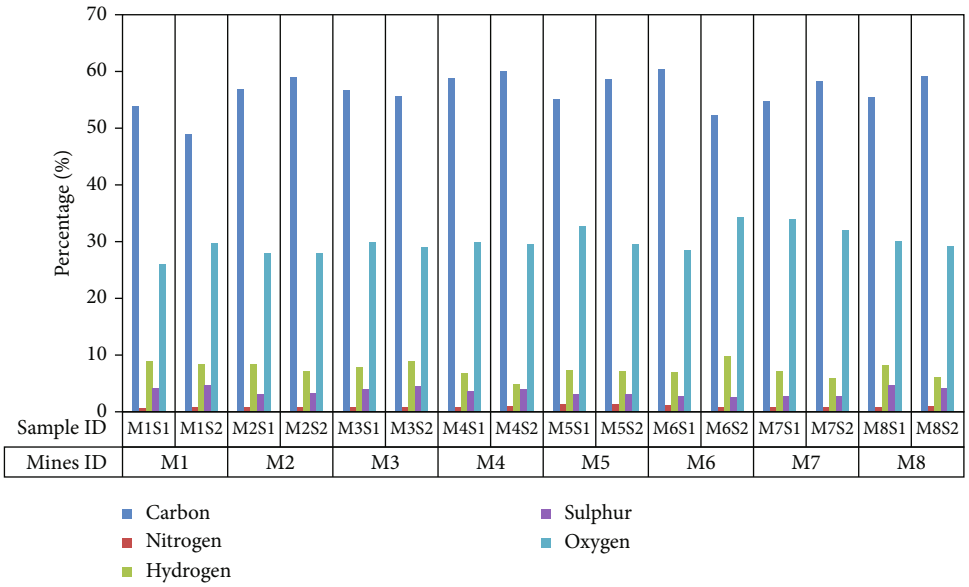

Figure 3: The elemental composition of the carbon, nitrogen, hydrogen, sulfur, and oxygen to find the sorption capacity and rank of Hangu Formation coal from different mines (M1-M8).

pores are mostly intergranular, dissolved pores, and tissue pores, partially filled with minerals. These pores are also connected with the microfractures developed during the coal-forming processes and can act as the main seepage channel.

It is assumed that the major episodes of these cleat patterns (face and butt cleats) are formed due to coalification and tectonic stresses. The cleat patterns in the coal samples indicate the compaction and dehydration of peat (coalification) during burial. These processes were the main reason for the shrinkage and caused the local tectonic stresses. Hence, the I2 irregular reticular subpattern is indicating the impact of tectonic stresses in the study area; whereas the samples from the deeper depth mines also consist of II2, isolated S subpatterns which are assumed to be formed under tectonic impact and shear stresses. These episodes helped to generate the cleats and their medium interconnectivity which contributes to the increase in porosity and permeability, whereas the intergranular pores are of different pore sizes and shapes which are developed due to diagenesis of various coal-forming materials. The dissolved pores are formed due to the dissolution of minerals which majorly include carbonates, quartz, and feldspar (Figure 4). The dissolved minerals can be the result of postdepositional processes such as the impact of compressional tectonic and trapped fluid and gases. The cleats and pore spaces can be helpful for the flow of methane in the Hangu Formation coal in the study area. However, the face and butt cleats (macrocracks) are also filled with minerals which majorly include quartz, calcite, and other minerals (Figure 4). These minerals are filled in the form of veins and are considered authigenic minerals. The minerals in the filled cleats generate the locally wider fractures due to effective stress in the study area.

It is assumed that the diagenesis of various coal-forming materials creates the pore spaces. The multiple mineral phases indicate that the cleats remained open over the long geological periods. Further, the tectonic influence in the study area causes the opening of cleats periodically and allows the fluid to migrate. The precipitation of authigenic minerals helped to maintain fracture porosity and enhance the ability to conduct fluid or gases. It is concluded that the cleat network and drying out within cleats are indicating large compaction during coalification which creates stresses and forms fractures. These fractures and pore spaces are ideal for methane accumulation and maintain reservoir permeability.

4.3. Identification of Pore Size and Its Surface Area. The storage matrix of methane consists of complex nanopore systems (micropore, mesopore, and macropore) and surface area, which has a direct impact on the sorption capacity of methane and acts as the interface between the methane and the coal seams. To keep this in mind, the representative samples (M1S1, M3S2, M4S1, and M6S1) were analyzed to identify the surface area and the pore geometry of Hangu Formation coal in the shallow and deeper depth mines. The samples M1S1 and M3S2 are from shallow depth mines, whereas the samples M4S1 and M6S1 are from deeper depth mines. During the analysis, the injection of N_2 gas experienced three pressure intervals having absorption at relatively low pressure ($<0.004 + e^{00}$). Once the adsorption ended, more N_2 was injected to find the adsorption capacity of each sample. Firstly, the nitrogen molecules disperse in the micropore at incredibly low pressure, adsorbed as condensing with relative precision continuously rising in the monolayer state and subsequent layers. The analysis indicates the higher adsorption capacity of studied coal with the increased surface area along with the cumulative pore volume, whereas the adsorption curves of the studied coal samples of the Makarwal area are of type II adsorption isotherm curve [57] indicating the physical adsorption of the N_2 gas on the micropore matrix (Figure 5). On the other hand, hysteresis loops are interpreted as the combination of type H3 and

>

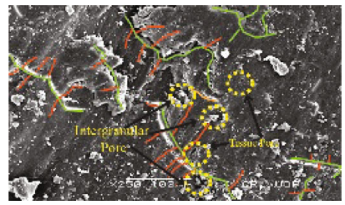

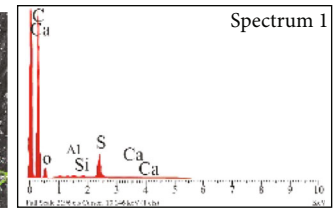

Element	Weight %
C K	77.42
O K	20.69
Al K	1.89
Totals	100

Legend

- Face cleat
- Butt cleat
- S type cleat
- Pore spaces
- C K: $CaCO_3$,
- O K: SiO_2
- Al K: Al_2O_3
- Si K: SiO_2
- S K: FeS_2
- K K: Feldspar
- Ca K: Wollastonatite
- Ti K: Titanium
- Fe K: Iron

(a)

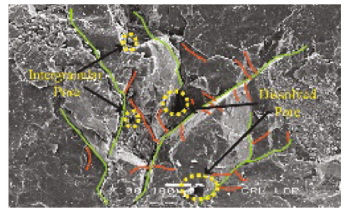

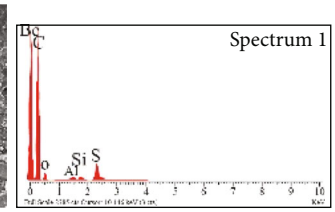

Element	Weight %
C K	82.11
O K	14.78
Al K	0.28
Si K	0.25
S K	2.57
Totals	100

Legend

- Face cleat
- Butt cleat
- S type cleat
- Pore spaces
- C K: $CaCO_3$,
- O K: SiO_2
- Al K: Al_2O_3
- Si K: SiO_2
- S K: FeS_2
- K K: Feldspar
- Ca K: Wollastonatite
- Ti K: Titanium
- Fe K: Iron

(b)

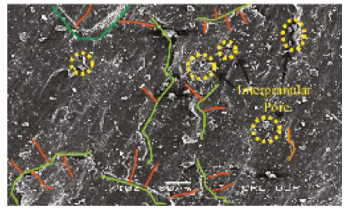

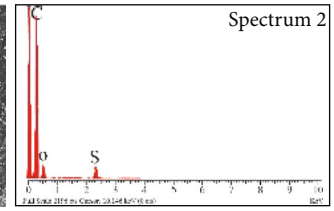

Element	Weight %
C K	81.68
O K	14.41
Al K	0.18
Si K	0.18
S K	3.44
Ca K	0.11
Totals	100

Legend

- Face cleat
- Butt cleat
- S type cleat
- Pore spaces
- C K: $CaCO_3$,
- O K: SiO_2
- Al K: Al_2O_3
- Si K: SiO_2
- S K: FeS_2
- K K: Feldspar
- Ca K: Wollastonatite
- Ti K: Titanium
- Fe K: Iron

(c)

Figure 4: Continued.

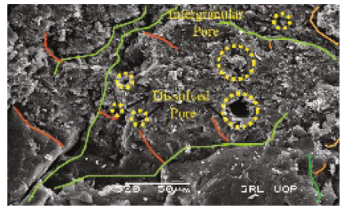

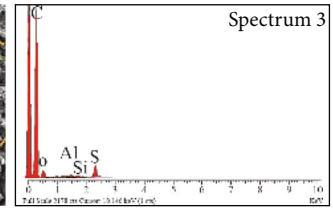

Element	Weight %
C K	83.74
O K	13.95
Al K	0.18
Si K	0.26
S K	1.88
Totals	100

Legend

- Face cleat
- Butt cleat
- S type cleat
- Pore spaces
- C K: $CaCO_3$,
- O K: SiO_2
- Al K: Al_2O_3
- Si K: SiO_2
- S K: FeS_2
- K K: Feldspar
- Ca K: Wollastonatite
- Ti K: Titanium
- Fe K: Iron

(d)

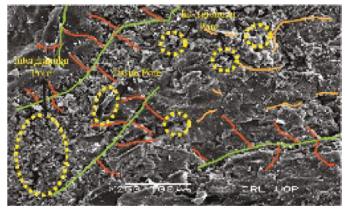

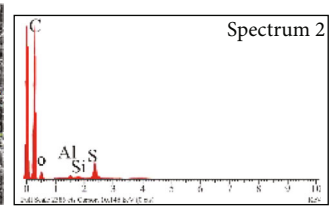

Element	Weight %
C K	82.70
O K	14.10
Al K	0.31
Si K	0.20
S K	2.69
Totals	100

Legend

- Face cleat
- Butt cleat
- S type cleat
- Pore spaces
- C K: $CaCO_3$,
- O K: SiO_2
- Al K: Al_2O_3
- Si K: SiO_2
- S K: FeS_2
- K K: Feldspar
- Ca K: Wollastonatite
- Ti K: Titanium
- Fe K: Iron

(e)

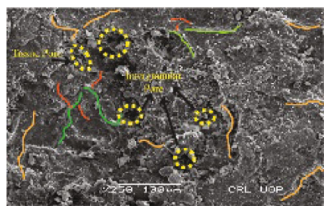

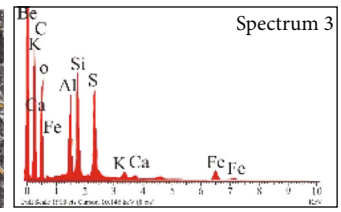

Element	Weight %
C K	61.20
O K	25.71
Al K	2.83
Si K	3.87
S K	3.74
K K	0.37
Ca K	0.22
Ti K	0.24
Fe K	1.81
Totals	100

Legend

- Face cleat
- Butt cleat
- S type cleat
- Pore spaces
- C K: $CaCO_3$,
- O K: SiO_2
- Al K: Al_2O_3
- Si K: SiO_2
- S K: FeS_2
- K K: Feldspar
- Ca K: Wollastonatite
- Ti K: Titanium
- Fe K: Iron

(f)

Figure 4: Continued.

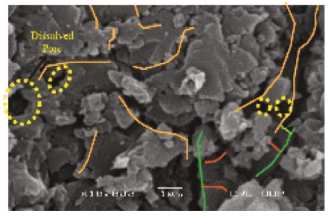

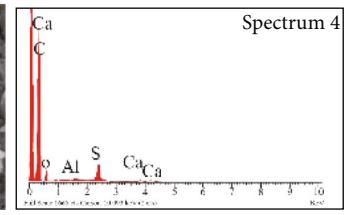

Element	Weight %
C K	80.94
O K	15.81
Al K	0.19
S K	2.84
Ca K	0.22
Totals	100

Legend

- Face cleat
- Butt cleat
- S type cleat
- Pore spaces
- C K: $CaCO_3$,
- O K: SiO_2
- Al K: Al_2O_3
- Si K: SiO_2
- S K: FeS_2
- K K: Feldspar
- Ca K: Wollastonatite
- Ti K: Titanium
- Fe K: Iron

(g)

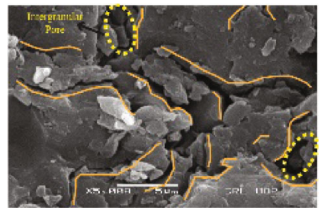

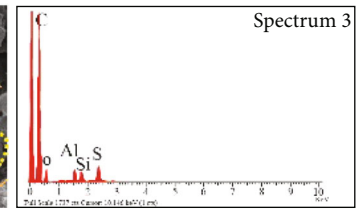

Element	Weight %
C K	77.01
O K	18.62
Al K	1.27
Si K	1.10
S K	2.00
Totals	100

Legend

- Face cleat
- Butt cleat
- S type cleat
- Pore spaces
- C K: $CaCO_3$,
- O K: SiO_2
- Al K: Al_2O_3
- Si K: SiO_2
- S K: FeS_2
- K K: Feldspar
- Ca K: Wollastonatite
- Ti K: Titanium
- Fe K: Iron

(h)

Figure 4: The SEM images and EDX analysis for the identification of cleat patterns, genetic type of pore classification, and mineral distribution within the cleats in the study area on different samples (a) M1S1, (b) M2S2, (c) M3S2, (d) M4S1, (e) M5S1, (f) M6S1, (g) M7S1, and (h) M8S1.

H4, which indicates the open cracks with well-developed micropores and their good connectivity [58].

The sample weight of M1S1 and M3S2 were 0.0896 g and 0.0585 g, whereas the volume of each sample is 0.02297 cc and 0.015 cc, respectively. According to the BET analysis, the surface area of both samples ranges between 69.612 m^2/g and 109.965 m^2/g (Figure 6). The pore volume of the M1S1 sample is 0.017 cc/g and the pore radius is 1.50 nm. However, the pore volume of M3S2 is 0.029 cc/g and the pore radius is 1.63 nm (Figure 6). On the other hand, the samples M4S1 and M6S1 of deeper depth mines consist of 0.0576 g and 0.066 g weights having the volume of 0.0147 cc and 0.0169 cc, respectively. The BET analysis indicates that the surface area of both samples ranges between 111.797 m^2/g and 109.641 m^2/g (Figure 6). However, the pore volume of M4S1 is 0.029 cc/g and the pore radius is 1.78 nm. Furthermore, the pore volume of M6S1 ranges 0.025 cc/g and its pore radius is 1.95 nm.

From the pore size analysis of the studied samples, it has been observed that the surface area in Makarwal coal samples varies from 69.61 to 111.79 m^2/g. However, the pore diameter is increasing from shallow to the deeper depth mine (Figures 6(a) and 6(b)). According to the International Union of Pure and Applied Chemistry (IUPAC) classification [59], the pores are classified as micropores (<2 nm), mesopores (2-50 nm), and macropores (>50 nm). Based on this classification, the Hangu Formation coal of the study area consists of micropore system. Furthermore, these pores act as the transitional pores and can be helpful in providing the transport pathways for the methane which can be stored in the adsorbed state. Hence, these adsorbed gases consist of 80-90% of the coal methane percentage [60]. Further, the H3 and H4 hysteresis loops suggested the relatively well-developed micropores with open cracks. The results indicating that such conditions are helpful for the gas flow in the pores of the studied samples.

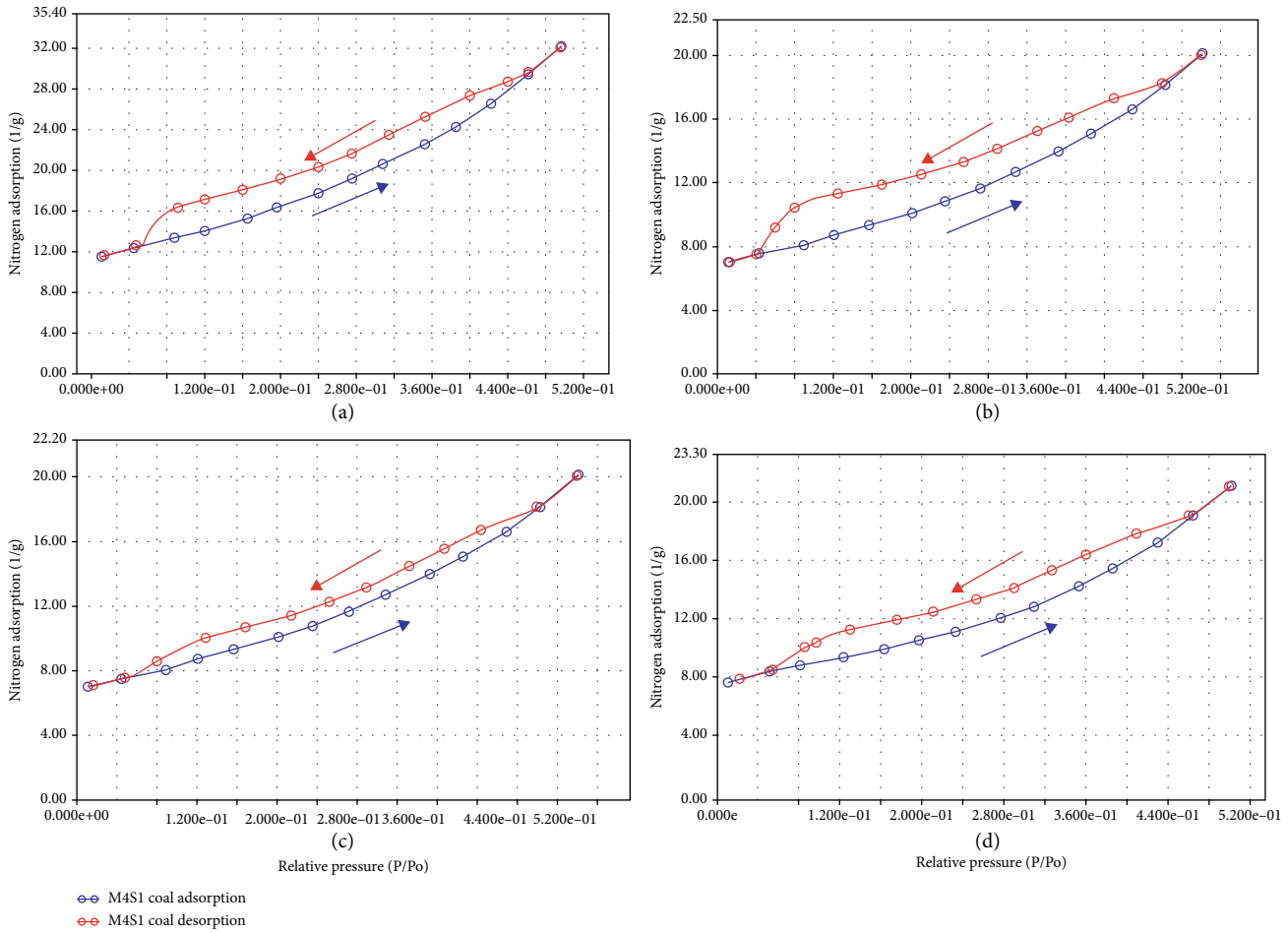

Figure 5: The nitrogen adsorption isotherms of selected coal samples (a) M1S1, (b) M3S2, (c) M4S1, and (d) M6S1 of Hangu Formation.

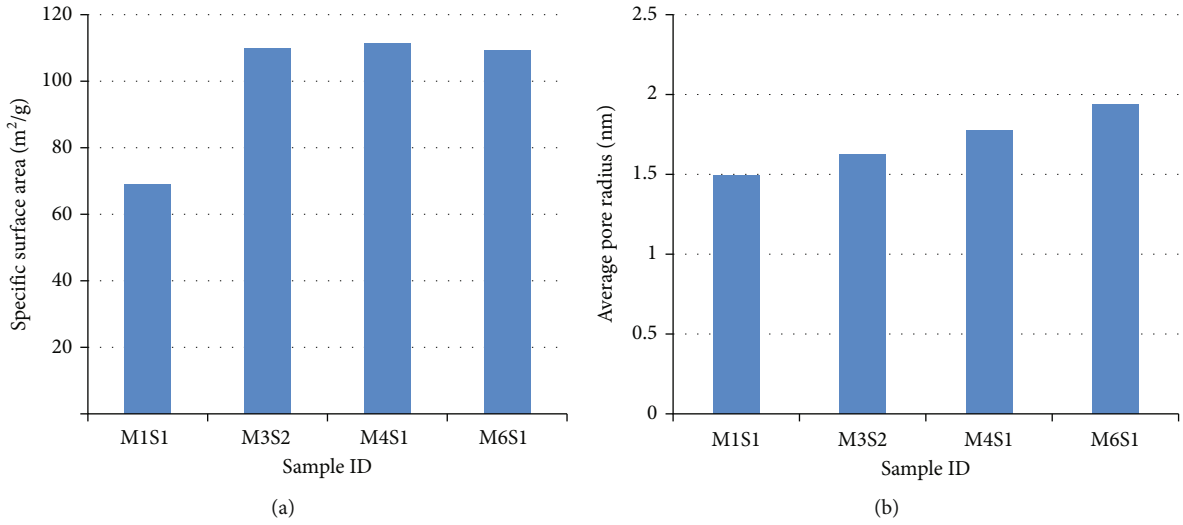

Figure 6: (a) The BET surface area and the (b) pore volume of the representative samples.

4.4. Mineralogical Identification. The brittle and ductile minerals associated with the Hangu Formation coal were evaluated to understand its drilling potential for the extraction of methane. For this purpose, the associated brittle minerals should be 50% wt. [61, 62]. The mineralogical peaks generated based on XRD analysis of representative samples are shown in Figures 7(a–7(d). The major minerals identified in all the samples are smectite, illite, kaolinite,

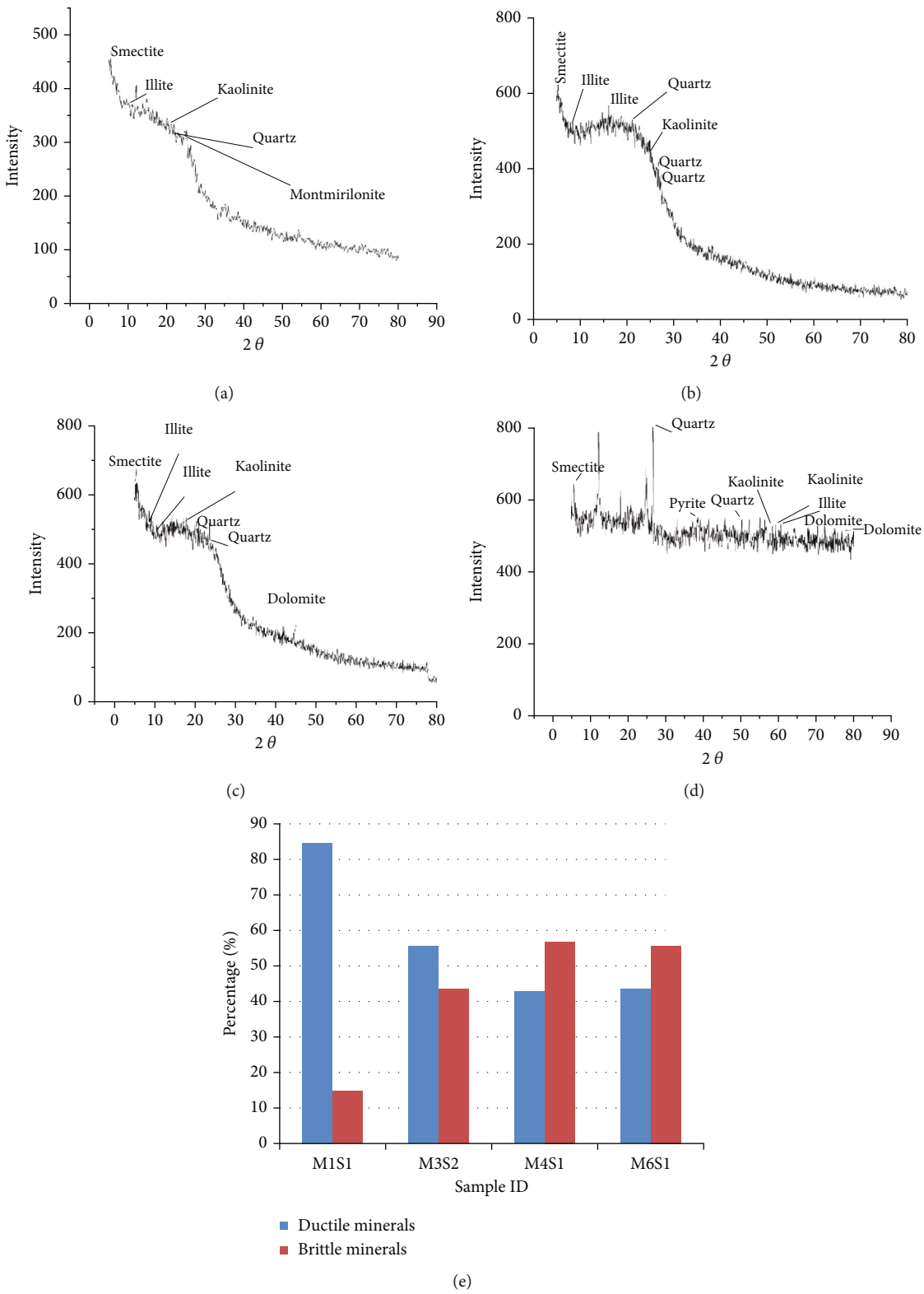

Figure 7: The XRD pattern of the Hangu Formation coal indicating minerals identified in (a) M1S1, (b) M3S2, (c) M4S1, and (d) M6S1 samples and (e) the presence of brittle and ductile minerals within the Hangu Formation coal.

montmorillonite, quartz, and dolomite. The clay minerals (smectite, illite, kaolinite, and montmorillonite) are the ductile minerals, whereas the quartz and dolomite are considered the brittle minerals. The shallow coal mine (M1) consists of majorly clay minerals and ranges up to 85%. However, it is decreasing towards the south (deeper coal

Table 1: The ductile and brittle minerals identification based on the XRD analysis.

Sample ID	Ductile minerals					Brittle minerals		
	Smectite (%)	Illite (%)	Kaolinite (%)	Montmorillonite (%)	*Total (%)*	Quartz (%)	Dolomite (%)	*Total (%)*
M1S1	22	18	32	13	**85**	15	0	**15**
M3S2	21	18	17	0	**56**	44	0	**44**
M4S1	19	19	15	0	**43**	46	11	**57**
M6S1	13	11	20	0	**44**	34	22	**56**

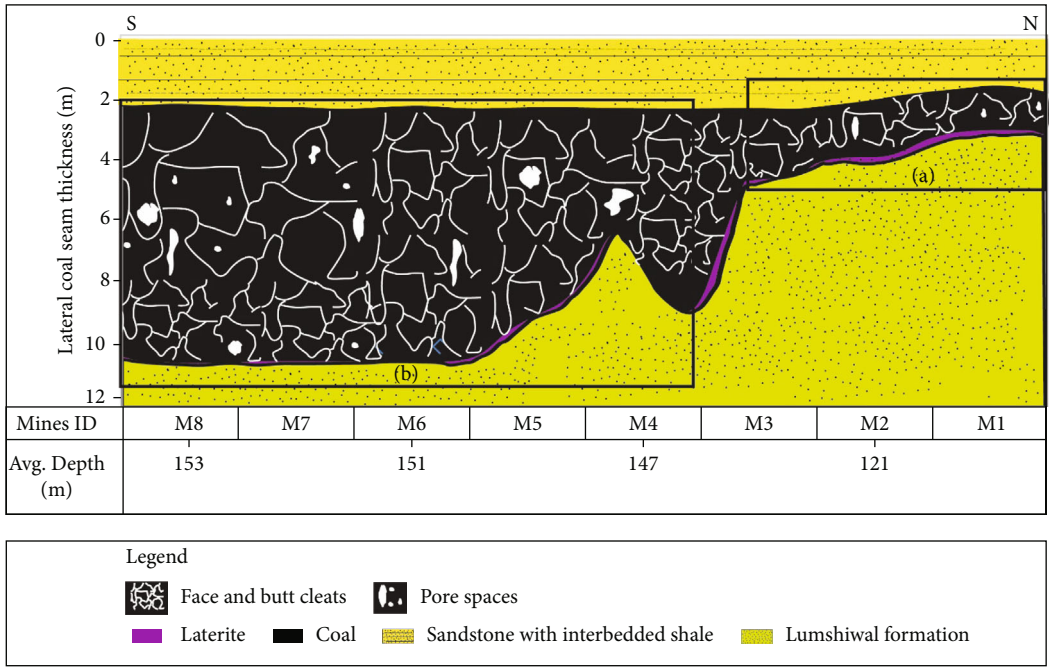

Figure 8: The model generated (a) shallow depth mines area and (b) deeper depth mine area on the basis of different analyses indicating the good potential of trapping of methane towards the south of the study area having good fracking abilities.

mines) and ranges up to 44% in mine M6 (Table 1). On the other hand, the brittle minerals are also increasing towards the south and reach up to 56%. The decrease in the ductile minerals and increase in the brittle minerals towards the south indicate the good potential of methane extraction in the south of the study area (Figure 7(e)). Hence, it is considered that the brittle minerals associated with coal seams experience lower permeability damage which is favorable for the better fracturing processes.

On the basis of above analyses, a model of coal seam with its lateral thickness of the study area is prepared (Figure 8). Overall, in the shallow depth mines towards the north consist of higher moisture, volatile matter, and ash contents. Further, the lower surface area of pores with less pore volume is not suitable for the trapping of methane in the cleat structures. On the other hand, the thickness of the coal seam is increasing towards the south. The increasing fixed carbon ratio, surface area, and pore volume with higher brittle minerals are ideal for the coalbed methane trapping and its extraction in the study area.

5. Conclusions

The proximate composition indicates that the carbon ratio and volatile matter is increasing, whereas moisture and ash content is decreasing towards the south (deeper depth) of the study area. Similarly, the ultimate analysis including the higher carbon and sulfur content with a lower hydrogen ratio is favorable for the higher adsorption capacity of gas in the coal seam of the Hangu Formation. Both analyses help to identify that the coal is ranked between bituminous and subbituminous, which is favorable for the generation of good internal cleat structures for gas storage, whereas the identified medium interconnected face and butt cleats, with the wide distribution of intergranular, dissolved and the tissue pore type generates the permeability and can be helpful in the flow of methane. The interpreted I2, irregular reticular subpattern, and II2, isolated S subpatterns, are representing the impact of tectonic and shear stresses in the study area. Hence, the cleat structures are partially filled with minerals demonstrating the cleats remained open over the long geological periods. It can be helpful to maintain fracture

porosity and enhance the ability to conduct fluid or gases. While the transitional micropore system identified in the coal samples is considered the primary mechanism for retaining gas due to adsorption in coalbeds. It acts as a transport pathway and can store gas in the adsorbed state. In addition, the higher surface area with cumulative pore volume enhanced the capacity of gas adsorption in the deeper depth. The type II adsorption isotherm curve indicates the adsorption potential of the Hangu Formation coal will easily trap free methane molecules and enhance its storage ability. Lastly, the Hangu Formation coal consists of both brittle and ductile minerals. The brittle minerals are increasing towards the south which is indicating the favorable conditions for the extraction of economical methane in the study area.

Data Availability

The data will be shared upon reasonable request from readers.

Conflicts of Interest

The authors declared no conflict of interest regarding the publication of this paper.

Acknowledgments

The authors would like to thank Universiti Teknologi Petronas, Malaysia, for the lab analysis and technical support at Geoscience Department and research funded YUTP-FRG 1/2021 015LC0-363. Moreover, special thanks are due to the Makarwal Collieries Limited, Pakistan, for accessing their mines and for conducting this research work. The laboratory facilitation provided by the Center of Coal Technology, Punjab University, Pakistan, and Centralized Resource Laboratory (CRL), University of Peshawar, Pakistan, are also highly appreciated.

References

[1] J. Zhang, L. Si, J. Chen, M. Kizil, C. Wang, and Z. Chen, "Stimulation techniques of coalbed methane reservoirs," *Geofluids*, vol. 2020, Article ID 5152646, 23 pages, 2020.

[2] L. Gao, M. Mastalerz, and A. Schimmelmann, "The origin of coalbed methane," in *Coal Bed Methane*, pp. 3–34, Elsevier, 2020.

[3] P. Thakur, "Global reserves of coal bed methane and prominent coal basins," in *Advanced Reservoir and Production Engineering for Coal Bed Methane*, pp. 1–15, Elsevier, 2017.

[4] Global Overview of CMM Opportunities, "US Environmental Protection Agency (US EPA) Coal bed methane outreach program," 2009, https://www.epa.gov/cmop.

[5] NAEWG, North American Natural Gas Vision Report, "North American energy working group experts group on natural gas trade and interconnections," 2005, https://www.energy.gov/articles/north-american-energy-work-group-releases-updated-trilateral-energy-report.

[6] K. Aminian, "Gas storage in coal," in *Coal Bed Methane*, pp. 115–131, Elsevier, 2020.

[7] Y. Cheng, H. Jiang, X. Zhang, J. Cui, C. Song, and X. Li, "Effects of coal rank on physicochemical properties of coal and on methane adsorption," *International Journal of Coal Science & Technology*, vol. 4, no. 2, pp. 129–146, 2017.

[8] C. F. Rodrigues, C. Laiginhas, M. Fernandes, M. J. Lemos de Sousa, and M. A. P. Dinis, "The coal cleat system: a new approach to its study," *Journal of Rock Mechanics and Geotechnical Engineering*, vol. 6, no. 3, pp. 208–218, 2014.

[9] B. Karmakar, T. Ghosh, K. Ojha, A. K. Pathak, and J. Devraju, "Effects of chemical composition and petrography of coal for coalbed methane evaluation with special reference to in-situ gas content," in *10th Biennial International Conference and Exposition*, Kochi, 2013.

[10] Z. Wang, J. Pan, Q. Hou, B. Yu, M. Li, and Q. Niu, "Anisotropic characteristics of low-rank coal fractures in the Fukang mining area, China," *Fuel*, vol. 211, pp. 182–193, 2018.

[11] Q. Li, D. Ma, Y. Zhang, Y. Liu, Y. Ma, and D. Hu, "Insights into controlling factors of pore structure and hydraulic properties of broken rock mass in a geothermal reservoir," *Lithosphere*, vol. 2021, article 3887832, no. Special 5, 2021.

[12] D. Ma, H. Duan, J. Zhang, X. Liu, and Z. Li, "Numerical simulation of water–silt inrush hazard of fault rock: a three-phase flow model," *Rock Mechanics and Rock Engineering*, vol. 55, no. 8, pp. 5163–5182, 2022.

[13] D. Ma, H. Duan, and J. Zhang, "Solid grain migration on hydraulic properties of fault rocks in underground mining tunnel: radial seepage experiments and verification of permeability prediction," *Tunnelling and Underground Space Technology*, vol. 126, article 104525, 2022.

[14] Y. Ye, S. Tang, and Z. Xi, "Brittleness evaluation in shale gas reservoirs and its influence on fracability," *Energies*, vol. 13, no. 2, p. 388, 2020.

[15] M. A. Zaib, A. Wahid, I. Siddiqui, S. H. Ali, B. A. Shami, and R. Q. Ahmed, "Identification and formation evaluation of unconventional shale gas: a case study of sembar formation, Southern Indus basin, Pakistan," in *Conference: SPE Annual Technical Conference, 14-15 December, 2021: Indigenous Resources and Energy Dynamics of Pakistan*, Islamabad, 2021.

[16] S. H. Ali, "Shale gas-an overview," in *2nd SEG Middle East Geoscience Student Symposium 28 April*, Poster Session, Muscat, Oman, 2014.

[17] S. H. Ali, "Pakistan shale gas candidates-an overview: a case study from lower Indus basin," in *1st DGS Students Symposium*, Poster Session, Al-Khobar, Saudi Arabia, 2014.

[18] M. H. Baloch, S. T. Chauhdary, D. Ishak et al., "Hybrid energy sources status of Pakistan: An optimal technical proposal to solve the power crises issues," *Energy Strategy Reviews*, vol. 24, pp. 132–153, 2019.

[19] M. S. Malkani, "A review of coal and water resources of Pakistan," *Journal of Science, Technology and Development*, vol. 31, no. 3, pp. 202–218, 2012.

[20] A. Nazeer, S. H. Shah, S. A. Abbasi, S. H. Solangi, and N. Ahmad, "An Overview of CBM resources in lower Indus basin, Sindh, Pakistan," *Earth Science*, vol. 6, no. 1, 2017.

[21] W. Danilchik and S. M. Shah, "Stratigraphy and coal resources of the Makarwal area, trans-Indus mountains, Mianwali district, Pakistan," *United States Geological Survey*, vol. 75, pp. 13–41, 1987.

[22] N. Rehman, D. S. H. Ali, Z. Ullah et al., "The evaluation of Khyber limestone in Pakistan for using as road aggregate based

on geotechnical properties," *Iranian Journal of Earth Sciences (Article in Press)*, vol. 2022, 2022.

[23] Q. Yasin, S. Baklouti, P. Khalid, S. H. Ali, C. D. Boateng, and Q. Du, "Evaluation of shale gas reservoirs in complex structural enclosures: a case study from Patala formation in the Kohat-Potwar plateau, Pakistan," *Journal of Petroleum Science and Engineering*, vol. 198, article 108225, 2021.

[24] S. Ghazi, S. H. Ali, T. Shahzad et al., "Sedimentary, structural and salt tectonic evolution of Karoli-Nilawahan area, central Salt Range and its impact for the Potwar Province," *Himalayan Geology*, vol. 41, no. 2, pp. 145–156, 2020.

[25] N. Ahmed, S. H. Ali, M. Ahmad et al., "Subsurface structural investigation based on seismic data of the north-eastern Potwar basin, Pakistan," *Indian Journal of Geo-Marine Sciences, Indian Journal of Geo-Marine Sciences*, vol. 49, no. 7, pp. 1258–1268, 2020.

[26] S. Ghazi, S. H. Ali, M. Sahraeyan, and T. Hanif, "An overview of tectonosedimentary framework of the Salt Range, northwestern Himalayan fold and thrust belt, Pakistan," *Arabian Journal of Geosciences*, vol. 8, no. 3, pp. 1635–1651, 2015.

[27] M. R. Shah, I. A. Abbasi, M. Haneef, and A. Khan, "Nature, origin and mode of occurrence of Hangu-Kachai area coal, district Kohat, NWFP, Pakistan: a preliminary study," *Geological Bulletin*, vol. 26, pp. 87–94, 1993.

[28] M. S. Malkani and Z. Mahmood, "Coal resources of Pakistan: entry of new coalfields," *Geological Survey of Pakistan, Information Release*, vol. 980, pp. 1–28, 2017.

[29] M. R. Shah, *Paleoenvironments, sedimentology and economic aspects of the Paleocene Hangu Formation in Kohat-Potwar and Hazara area, [Ph.D. thesis]*, University of Peshawar, Peshawar, 2001.

[30] I. Ahmad, S. Ahmad, and F. Ali, "Structural analysis of the Kharthop and Kalabagh Hills area, Mianwali district, Punjab, Pakistan," *Journal of Himalayan Earth Science*, vol. 49, no. 2, pp. 63–74, 2016.

[31] A. Ali, *Structural analysis of the Trans-Indus Ranges: implications for the hydrocarbon potential of the NW Himalayas, Pakistan, [Ph.D. thesis]*, National Centre of Excellence in Geology University Of Peshawar, Pakistan, 2010.

[32] A. Mateen, A. Wahid, H. T. Janjuhah et al., "Petrographic and geochemical analysis of Indus sediments: implications for placer gold deposits, Peshawar Basin, NW Himalaya, Pakistan," *Minerals*, vol. 12, no. 8, p. 1059, 2022.

[33] S. H. Ali, *Reservoir characteristics of early-Middle Cambrian Baghanwala Formation, Eastern Salt Range Pakistan, SPE and PAPG annual technical conference, maximize reserves–optimize exploitation, November 17-18*, Serena Hotel, Islamabad, 2009.

[34] J. W. McDougall and S. H. Khan, "Strike-slip faulting in a foreland fold-thrust belt: the Kalabagh Fault and Western Salt Range, Pakistan," *Tectonics*, vol. 9, no. 5, pp. 1061–1075, 1990.

[35] A. Wahid, A. Rauf, S. H. Ali, J. Khan, M. A. Iqbal, and A. Haseeb, "Impact of complex tectonics on the development of geo-pressured zones: a case study from petroliferous sub-Himalayan basin," *Geopersia*, vol. 12, no. 1, pp. 89–106, 2021.

[36] A. Javed, A. Wahid, M. S. Mughal et al., "Geological and petrographic investigations of the Miocene Molasse deposits in sub-Himalayas, district Sudhnati, Pakistan," *Arabian Journal of Geosciences*, vol. 14, no. 15, pp. 1–24, 2021.

[37] F. Ali, M. I. Khan, S. Ahmad, G. Rehman, I. Rehman, and T. H. Ali, "Range front structural style: an example from Surghar Range, North Pakistan," *Journal of Himalayan Earth Sciences*, vol. 47, no. 2, p. 193, 2014.

[38] I. Alam, A. M. Azhar, and M. W. Khan, "Frontal structural style of the Khisor Range, northwest of Bilot: implications for hydrocarbon potential of the North-Western Punjab foredeep, Pakistan," *Journal of Himalayan Earth Science*, vol. 47, no. 1, p. 14, 2014.

[39] M. S. Malkani, Z. Mahmood, S. I. Shaikh, and M. I. Alyani, "Mineral resources of north and South Punjab, Pakistan," *Geological Survey of Pakistan, Information Release*, vol. 995, pp. 1–52, 2017.

[40] K. A. Qureshi, M. R. Shah, I. A. Meerani, S. Fahad, H. Hussain, and U. Habib, "Sedimentology and economic significance of Hangu formation, Northwest Pakistan," *International Journal of Economic and Environmental Geology*, vol. 11, no. 1, pp. 48–55, 2020.

[41] I. A. Abbasi, M. Haneef, and M. A. Khan, "Early Permian siliciclastic system of the north Gondwanaland: a comparison between the Nilawahan group of North Pakistan and Haushi group of Oman," *Pakistan Journal of Hydrocarbon Research*, vol. 21, pp. 19–33, 2011.

[42] H. G. Reading, *Sedimentary environment and facies*, Blackwell Scientific Publication, 2nd edition, 1986.

[43] S. Iqbal, I. U. Jan, and M. Hanif, "The Mianwali and Tredian formations: an example of the triassic progradational deltaic system in the low-latitude western Salt Range, Pakistan," *Arabian Journal for Science and Engineering*, vol. 39, no. 7, pp. 5489–5507, 2014.

[44] I. A. Abbasi and R. McElroy, "Thrust kinematics in the Kohat plateau, Trans Indus Range, Pakistan," *Journal of Structural Geology*, vol. 13, no. 3, pp. 319–327, 1991.

[45] H. M. Z. Ali and S. Khan, "Ranking of Paleocene age coal salt range, Punjab and its application in coal fired power plants," *Science International*, vol. 27, no. 2, pp. 1243–1246, 2015.

[46] American Society for Testing and Materials, "Standard specifications for the classifications of coal by rank (ASTM designation D388-66), in gaseous fuels; coal and coke," *American Society for Testing Materials*, vol. 19, pp. 73–78, 1967.

[47] K. M. Czajka, N. Modliński, A. M. Kisiela-Czajka, R. Naidoo, S. Peta, and B. Nyangwa, "Volatile matter release from coal at different heating rates -experimental study and kinetic modelling," *Journal of Analytical and Applied Pyrolysis*, vol. 139, pp. 282–290, 2019.

[48] H. L. Lin, K. J. Li, X. W. Zhang, and Y. L. Li, "Structural characterization of ShendongShangwan coal and its maceral," *Coal Conversion*, vol. 36, pp. 1–5, 2013.

[49] S. Hao, J. Wen, X. Yu, and W. Chu, "Effect of the surface oxygen groups on methane adsorption on coals," *Applied Surface Science*, vol. 264, pp. 433–442, 2013.

[50] F. Zhou, S. Liu, Y. Pang, J. Li, and H. Xin, "Effects of coal functional groups on adsorption microheat of coal bed methane," *Energy & Fuels*, vol. 29, no. 3, pp. 1550–1557, 2015.

[51] X. Su, Y. Feng, J. Chen, and J. Pan, "The characteristics and origins of cleat in coal from Western North China," *International Journal of Coal Geology*, vol. 47, no. 1, pp. 51–62, 2001.

[52] J. Yue, Z. Wang, J. Chen, M. Zheng, Q. Wang, and X. Lou, "Investigation of pore structure characteristics and adsorption characteristics of coals with different destruction types," *Adsorption Science & Technology*, vol. 37, no. 7-8, pp. 623–648, 2019.

[53] M. E. Tucker, *Techniques in Sedimentology*, Blackwell Scientific Publications, 1988.

[54] Y. Yao, D. Liu, D. Tang, S. Tang, Y. Che, and W. Huang, "Preliminary evaluation of the coalbed methane production potential and its geological controls in the Weibei Coalfield, Southeastern Ordos Basin, China," *International Journal of Coal Geology*, vol. 78, no. 1, pp. 1–15, 2009.

[55] H. Susanto, K. Sondakh, R. Sitaresmi, and R. Hananda, "Evaluation of initial gas volume of coalbed methane using four method," *Journal of Mechanical Engineering and Mechatronics*, vol. 3, no. 1, pp. 28–39, 2019.

[56] Z. P. Meng, S. S. Liu, B. Y. Wang, Y. D. Tian, and J. Wu, "Adsorption capacity and its pore structure of coals with different coal body structure," *Journal of China Coal Society*, vol. 40, no. 8, pp. 1865–1870, 2015.

[57] Y. Yuan, Y. Tang, Y. Shan, J. Zhang, D. Cao, and A. Wang, "Coalbed methane reservoir evaluation in the Manas mining area, southern Junggar Basin," *Energy Exploration & Exploitation*, vol. 36, no. 1, pp. 114–131, 2018.

[58] S. Fu, Q. Fang, A. Li et al., "Accurate characterization of full pore size distribution of tight sandstones by low-temperature nitrogen gas adsorption and high-pressure mercury intrusion combination method," *Energy Science and Engineering*, vol. 9, no. 1, pp. 80–100, 2021.

[59] M. Thommes, K. Kaneko, A. V. Neimark et al., "Physisorption of gases, with special reference to the evaluation of surface area and pore size distribution (IUPAC technical report)," *Pure and Applied Chemistry*, vol. 87, no. 9-10, pp. 1051–1069, 2015.

[60] X. Zhang, P. Ranjith, M. Perera, A. S. Ranathunga, and A. Haque, "Gas transportation and enhanced coalbed methane recovery processes in deep coal seams: a review," *Fuels*, vol. 30, no. 11, pp. 8832–8849, 2016.

[61] Q. R. Passey, K. M. Bohacs, W. L. Esch, R. Klimentidis, and S. Sinha, "From oil-prone source rock to gas-producing shale reservoir–geologic and petrophysical characterization of unconventional shale-gas reservoirs," in *International oil and gas conference and exhibition in China*, Beijing, China, 2010.

[62] B. Katz, L. Gao, J. Little, and Y. R. Zhao, "Geology still matters - unconventional petroleum system disappointments and failures," *Unconventional Resources*, vol. 1, pp. 18–38, 2021.